IEEE Access
Multidisciplinary | Rapid Review | Open Access Journal

Received March 5, 2021, accepted April 25, 2021, date of publication May 4, 2021, date of current version May 13, 2021.

Digital Object Identifier 10.1109/ACCESS.2021.3077529

Natural Brain-Inspired Intelligence for Screening in Healthcare Applications

MAHDI NAGHSHVARIANJAHROMI[1], (Student Member, IEEE), SUMIT MAJUMDER[1], (Graduate Student Member, IEEE), SHIVA KUMAR[1], (Member, IEEE), NARJES NAGHSHVARIANJAHROMI[2], AND M. JAMAL DEEN[1], (Life Fellow, IEEE)

[1]Department of Electrical and Computer Engineering, McMaster University, Hamilton, ON L8S 4K1, Canada
[2]Department of Obstetrics and Gynecology, Jahrom University of Medical Sciences, Jahrom 74148-46199, Iran

Corresponding author: M. Jamal Deen (jamal@mail.ece.mcmaster.ca)

This work was supported in part by the Natural Sciences and Engineering Research Council (NSERC), and in part by the Canada Research Chair Program (CRCP).

ABSTRACT In recent years, there has been a growing interest in smart e-Health systems to improve people's quality-of-life by enhancing healthcare accessibility and reducing healthcare costs. Continuous monitoring of health through the smart e-Health system may enable automatic diagnosis of diseases like Arrhythmia at its early onset that otherwise may become fatal if not detected on time. In this work, we developed a cognitive dynamic system (CDS)-based framework for the smart e-Health system to realize an automatic screening process in the presence of a defective or abnormal dataset. A defective dataset may have poor labeling and/or lack enough training patterns. To mitigate the adverse effect of such a defective dataset, we developed a decision-making system that is inspired by the decision-making processes in humans in case of conflict-of-opinions (CoO). We present a proof-of-concept implementation of this framework to automatically identify people having Arrhythmia from single lead Electrocardiogram (ECG) traces. It is shown that the proposed CDS performs well with the diagnosis errors of 13.2%, 9.9%, 6.6%, and 4.6%, being in good agreement with the desired diagnosis errors of 25%, 10%, 5.9%, and 2.5%, respectively. The proposed CDS algorithm can be incorporated in the autonomic computing layer of a smart-e-Health-home platform to achieve a pre-defined degree of screening accuracy in the presence of a defective dataset.

INDEX TERMS Autonomic decision-making system, autonomic computing layer, cognitive dynamic system (CDS), cognitive decision making (CDM), non-Gaussian and non-linear environment, NGNLE, screening, smart systems, defective dataset, e-health, smart home, conflict of opinions.

I. INTRODUCTION

Currently, the autonomic decision-making systems (ADMS) [1]–[3] for smart interactive cyber-physical systems (CPS) are attracting much attention from researchers and technology providers [1]–[7]. The CDS is inspired by the neuroscience model of the human brain presented in [8] and it is built on the principles of cognition, i.e., perception-action cycle (PAC), memory, attention, intelligence, and language [9]–[16]. CDS has found applications in the smart home [3], [9], smart e-Health home [3], [10], and long-haul fiber-optic link [11]–[15]. It is proposed as an alternative to typical artificial intelligence (AI) methods for many AI applications [16]. In this paper, we present a cognitive dynamic system (CDS) for the screening process in smart e-Health systems based on the perception and multiple action cycles (PMAC) and the decision-making processes in humans in case of a conflict of opinion (CoO).

The algorithmic presentation of a CDS reported in [16] was based on linear and Gaussian environments (LGEs). However, health-related physiological data, which are measured to assess health conditions are generally not normally distributed, *i.e.* they are non-Gaussian [17], [18]. Moreover, most features extracted from the measured physiological signals vary in a non-linear manner with the human health condition. Therefore, human health and smart e-Health systems can be considered as non-Gaussian and non-linear health environments (NGNLHEs) as reported in the case of breast

The associate editor coordinating the review of this manuscript and approving it for publication was Qichun Zhang.

cancer modeling in [18]. In a NGNLHE healthcare system, the outputs are not linearly dependent on the inputs. Furthermore, the outputs of such a system do not follow Gaussian distributions.

In [11]–[15], a CDS was proposed for smart fiber optic communication systems to demonstrate its high precision decision-making ability in complex smart systems. It should be noted that we use the term cognitive decision making (CDM) to define decision making using CDS. The CDS was presented in [10]–[15] as an enhanced-AI that exploited the maximum probability (MAP) approach for the CDM. The CDS thus implemented resulted in a high-performance CDM, which however used a reliable dataset to train the model. When the datasets are not reliable due to poor labeling and/or insufficient training patterns defective or abnormal, the PAC-based CDS cannot perform well enough to satisfy requirements to provide reliable results for predefined healthcare policy. This can be explained with an analogy to the decision-making process of the human brain when it makes a judgment based on some ambiguous information, thus running a risk of making a wrong decision. In this paper, we propose a CDS algorithm to realize a reliable screening method in a smart e-Health system from a defective dataset. Here, we exploited the concept of CoO to realize the CDM for the NGNLHE system. We also generalized the concept of PAC in the PAC-based CDS to perception-multi actions cycles (PMAC) to implement the CoO.

The basic model of a CDS based on PMAC is presented in Fig. 1. There are three main subsystems in a CDS: (1) Perception by the Perceptor; (2) a Feedback channel for sending the multiple raw internal rewards; and (3) the Executive to perform multiple actions on the environment.

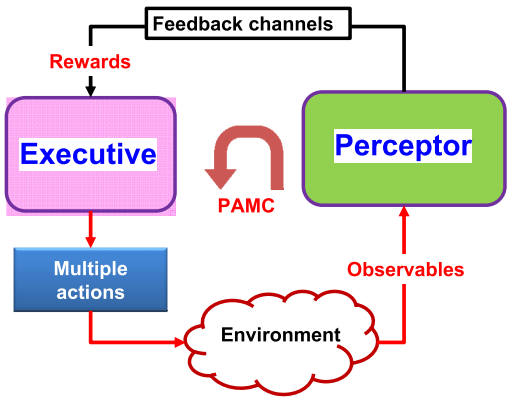

FIGURE 1. Block diagram of a cognitive dynamic system (CDS) based-on PMAC: Perception multiple actions cycle.

The main contributions of this work can be summarized as follows:

1) The PAC-based CDS for the NGNLHE based on MAP CDM [10]–[15] is enhanced as the proposed CDS with the PAC and CoO-based CDM for the screening process. This improvement allows for the mitigation of screening inaccuracies due to a defective dataset.
2) The structure of a PMAC-based CDS is designed as the first stage of the screening process. In this paper, we aim to screen human health condition automatically between two binary (healthy and unhealthy) states based on subjects' single lead ECG traces. We implemented a CoO-based CDM in the second stage to achieve a desired level of diagnosis error at an acceptable, high false alarm rate. The first stage was based on the diagnostic test or low false alarm policy presented in [10] using a PAC-based CDS.
3) Algorithms for decision making between healthy and unhealthy conditions in a NGNLE system is presented based on the screening process.
4) A proof-of-concept case study is presented in which a PMAC-based CDS is applied to screen for Arrhythmia from a defective dataset. It is shown that the proposed CDS performs well, giving good agreement with the desired diagnosis errors of 25%, 10%, 5.9%, and 2.5%, achieving average final diagnosis errors of 13.2%, 9.9%, 6.6%, and 4.6%, respectively. These diagnosis errors correspond to a clinically acceptable false alarm rates [19] of 20.1%, 25%, 28.4%, and 54.7% respectively, even with a defective dataset.

II. RELATED WORKS

In this section, we present a brief review of related works based on machine learning (ML) or artificial intelligence (AI) techniques. These techniques are widely used in decision making or false alarm reduction in healthcare applications [21]–[43]. Recently, owing to the increasing popularity of wearable and portable health sensors, a large number of health-related databases were developed [20]. To predict clinical outcomes or identify clinical problems from available datasets, clinicians, and researchers have a growing interest in using machine learning and AI techniques [21]. Also, machine learning is being used in the diagnosing of various diseases such as diabetic retinopathy [22], skin cancer [23] and prostate cancer [24], [25]. Furthermore, these techniques can also be used for optimizing disease treatment, control and decision making [26]–[28].

In [29], a machine learning technique was used to reduce false alarm rates in detecting Arrhythmia from the electro-cardiogram (ECG) signals. Machine learning techniques were also used to generate reports from medical images [30], [31]. In ML-based techniques, a generalized prediction model is developed from an initial set of data that subsequently allows for extracting patterns from the measured data. These extracted patterns may help medical doctors (MDs) to perform more personalized clinical prediction and plan customized intervention strategies [32].

Machine learning techniques are applied for specific healthcare screening applications. For example, deep learning was used for breast-cancer screening using mammography [33] or screening the glaucoma progression [34], [35]. Also, semi-supervised learning was used for screening glaucoma progression [36]. Machine learning was also used

for screening diabetic retinopathy and other ocular findings using telemedicine in [37]. In addition, ML can be used for early detection or screening of autism [38]–[40]. Furthermore, ML can use walking patterns to screen elderly health issues [41]–[42]. Applications of AI/ML were discussed in [43] for disease classification. Moreover, ref. [43] provided two limitations of AI/ML regarding implementation for healthcare applications. First, the ML performances depend on the dataset, and poor ML performances are results from the defective datasets. On the other hand, the dataset contains observations and measurement errors, or artifacts can result in poor results. Second, AI has a major challenge in the context of brain-inspired/biomedical decision-making: the typical AI reasoning step should be visible to the medical doctors and clinician, so they can interpret in an intelligible way. However, typically, AI algorithms lead to complex information processing and reasoning steps that may not be understandable to a human. Especially, the ML algorithm may learn complex rules, which results in good accuracy. However, it is very difficult for even a healthcare expert to understand these processing and reasoning steps and rules. In this paper, we presented PMAC-based CDS as a brain-inspired using CoO-decision making to mitigate AI/ML limitation in presence of defective datasets. Also, our proposed system can improve the understanding of the reasoning procedure of the algorithm for medical doctors using semi-human decision making with PMAC, CoO, and posterior extraction.

III. WHY A COGNITIVE DYNAMIC SYSTEM?

In this section, we present a brief discussion on conventional machine learning approaches and how CDS can become an efficient alternative to them. Machine learning approaches are generally employed in AI to build intelligent machines. This ML-based AI is however different from the symbolic rule-based AI. Unlike the rule-based AI, where decisions are made based on some predefined rules, ML-based AI learns from annotated classified datasets, examples, and experiences. In ML-based AI, a model is developed based on the information from the dataset, when it used for prediction. Also, the algorithm can learn to optimize models based on the dataset and policies for a specific task, for example, a screening process with an acceptable high false alarm policy.

A. MACHINE LEARNING APPROACHES

Machine learning enables some degree of intelligence in machines by extracting and using the information about patterns in datasets, examples, and experiences. There are several, machine learning approaches such as supervised learning, reinforcement learning, semi-supervised learning, unsupervised learning, and transfer learning. However, we will focus on two approaches that are more relevant to this work i.e. supervised learning and reinforcement learning.

1) SUPERVISED LEARNING

A popular approach in machine learning for practical applications such as predicting recovery time, medication response and health condition, is supervised learning (SL) because, it can find patterns present in the dataset. In general, the SL algorithm learns from the dataset (input predictors x) to create a classifier to predict the output response y. The SL algorithm extracts a mapping function f where $y = f(x)$. An algorithm with a set of input data $\{x_1, x_2, \ldots, x_n\}$ builds the classifier, which outputs $\{y_1, y_2, \ldots, y_n\}$ in response to the corresponding inputs (Fig. 2a).

Supervised learning can be divided into two main branches: (1) learning prediction and (2) learning by modeling. The first category of SL-based prediction can be divided into regression or classification problems. To estimate the values of the response, regression learning methods are more suitable whereas, algorithms such as logistic regression, naive Bayes, decision trees or support vector machines (SVM) are more useful for classification [44]. In the second category of SL, a predictive discriminative model is extracted using ML approaches such as decision trees and SVM algorithms which determine the decision boundaries within the data based on the learning objective. In the case of machine learning methods such as naive Bayes or Bayesian approaches, the model

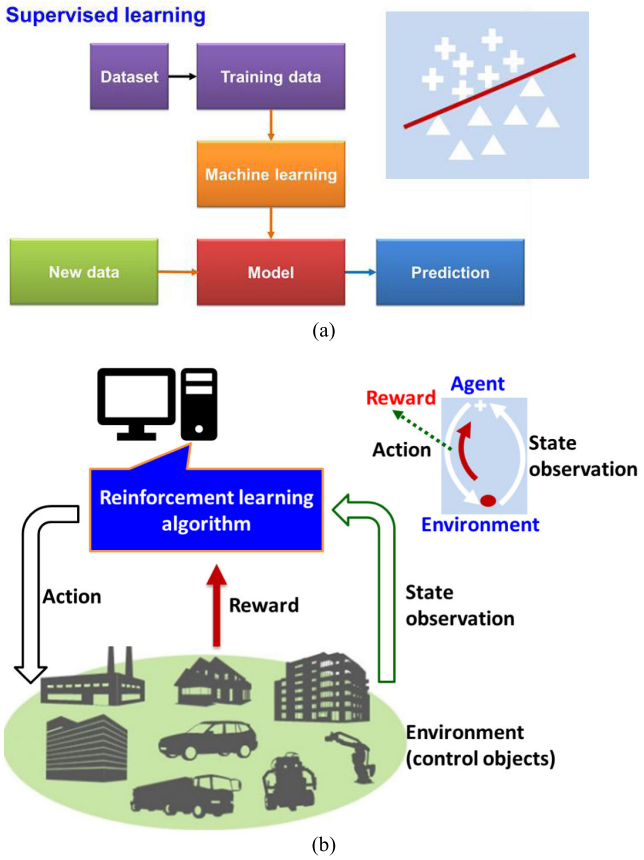

FIGURE 2. Schematic of two popular machine learning approaches (a) supervised learning (SL) (b) reinforcement learning (RL).

makes predictions by learning the probability distributions of the data.

In summary, the SL algorithm builds a predictive model from a labeled database. This model can then be used to estimate or classify the output in response to a new set of input data. Supervised learning algorithms are used in prediction and classification problems, such as in image recognition or filtering of spam emails (Fig. 2a).

2) REINFORCEMENT LEARNING

Reinforcement learning (RL) resolves a decision-making problem by learning and evolving through a trial-and-error approach (Fig. 2b), realized by the interaction between a computing agent and a dynamic environment [45]. While searching in the state-action space, the computing agent attempts to reach the highest reward (or lowest penalty) based on the feedback received from the dynamic environment. For example, in healthcare applications, the RL algorithm tries to improve the model parameters by iteratively simulating the states e.g. a user health's condition. Then, after applying the action (e.g. activating or deactivating sensors, amount of medication delivery, or modeling accuracy), the computing agent obtains the feedback reward from the environment (healthy or unhealthy - decision made by the MDs in the clinic). The RL algorithm finally converges to a model that may generate optimal decisions [16]. Unlike the SL algorithm, RL algorithms typically do not require a prior database and can automatically find the most appropriate actions by optimizing the feedback reward/penalty received from the dynamic environment.

B. CDS IMPLEMENTATION USING ML APPROACHES

In the earlier implementations of CDS [10]–[15], the PAC was realized by combining conventional ML approaches, such as RL, and SL. Here, we focus on how a PAC-based CDS and the proposed CDS in this paper can overcome weaknesses of SL and RL.

1) TYPICAL PAC-BASED CDS

A PAC-based CDS can be implemented by combining both SL and RL techniques of conventional machine learning. Figure 3 shows the block diagram of a PAC-based CDS for the healthcare environment. The Perceptor of the CDS can extract a model using the SL algorithm. The Perceptor then generates an internal reward and predicts the outcome of the dynamic environment (human health in this case) using the extracted model [16]. The Executive receives the internal reward from the Perceptor through the feedback channel. The Executive is built upon an RL-based ML approach that based on the internal reward in the current PAC finds an action, which can optimize the internal reward for the next PAC. The internal reward gives the CDS self-awareness, self-consciousness, and independence from the dynamic environment (Fig. 3).

In short, the RL-based Executive of a PAC-based CDS uses the internal reward produced by the model extracted in the SL-based Perceptor to apply a cognitive action on the

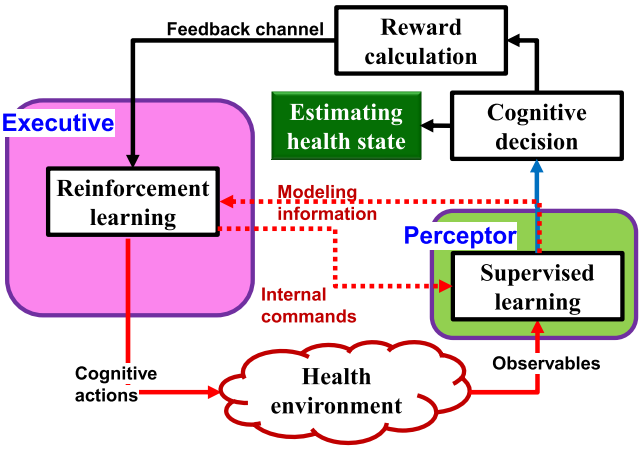

FIGURE 3. Conceptual implementation of PAC-based CDS.

dynamic environment. Therefore, a PAC-based CDS can be considered as an enhanced AI.

In typical RL, the agent applies the actions on a trial and error basis to receive feedback from the environment, whereas the CDS has a "*conscience*" about the actions. Therefore, the CDS is a more appropriate choice in intelligent machine applications, especially to ensure safety and security in healthcare applications.

2) PROPOSED PMAC-BASED CDS

In a typical PAC, the CDS applies an action on the environment and then uses the calculated reward (internal/external) to gain experience. The RL in the Executive then optimizes the reward in the following PAC by finding the most appropriate action. As mentioned before, the Perceptor of a PAC-based CDS uses SL to extract a model of the environment that requires a well-labeled dataset with enough number of training patterns to enhance the reliability of the model. For example, in the case of orthogonal frequency division multiplexing (OFDM) long-haul fiber optic communication systems [11]–[15] when the CDS operates in the bit error rate (BER) improvement mode, the internal rewards and model converges after $N = 512$ frames.

Unlike fiber-optic communications, where training data with accurate labeling are available at a much faster rate, the number of training patterns in the available datasets for healthcare applications is generally limited. In addition, the labeling of the healthcare dataset can be erroneous owing to its dependence on human skills. Moreover, a dataset can be inherently defective or manipulated by hidden cyber-attack. These shortcomings in the available data may result in an overfitted model, potentially causing the test accuracy of the model to drop significantly compared to the training accuracy. In such a case, one can infer that the used dataset for model extraction is badly labeled and/or lacks enough training patterns required to extracting a reliable, accurate and converged model. Without a converged model in a PAC-based CDS, the SL-based perception process based on PAC and

internal reward generation can limit the accuracy and consistency of the performance of the Executive in the case of healthcare applications.

In this paper, we extended the typical PAC to the proposed PMAC (Fig. 4) in an attempt to mitigate the inherent deficiency of SL. In the PMAC-based CDS, the Executive applies multiple actions simultaneously on the health environment in one cycle, for example, activates different ECG leads, or the Photoplethysmogram (PPG) sensor. The Perceptor receives new measurements from the environment to extract model(s) and uses the model(s) to generate multiple raw internal rewards for the Executive. In the following cycle, the Executive performs multiple actions on the environment to optimize each internal reward based on some pre-defined policies by the users. The Executive also provides weighted internal rewards using the cost-to-go-functions based on the received raw internal rewards through the feedback channels. These weighted internal rewards can be used by the CoO for CDM (Fig. 4).

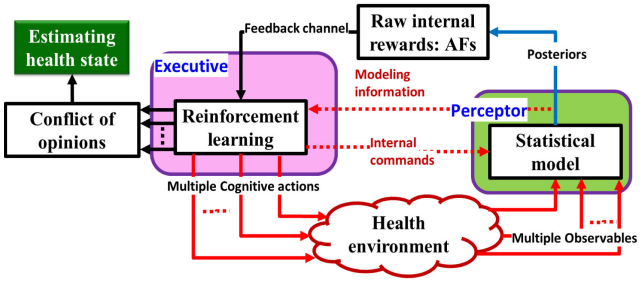

FIGURE 4. Conceptual implementation of PMAC based CDS.

For the screening process, the PAC-based CDS initially assumes that the user is 'Unhealthy'. In the case of a 'Healthy' user, the CDS applies some actions on the environment (user body) and finds the relevant evidence of the user being 'Healthy'. Then, the CDS feeds the evidence i.e. the newly measured parameters from the environment (user body) into the extracted model in the Perceptor and changes the decision about the user's health state to 'Healthy'. Similar to the PAC-based CDS, the PMAC-based CDS also assumes an 'Unhealthy' state as the initial decision for the user's health. However, unlike the PAC-based CDS, the Executive of the PMAC-based CDS applies two actions simultaneously for two states - 'Healthy' and 'Unhealthy' - on the environment (user body), to find evidence in favor of each state separately.

In the case of conflicting outcomes, when the CDS has evidence in favor of both states, the amount of evidence in favor of a particular state plays a crucial role in resolving the conflict in decision making. For example, 100 evidence in favor of 'Healthy' state with 99% assurance provides a final reward of 99, while 105 evidence in favor of 'Unhealthy' state with 95% assurance results in a final reward of 99.75. Thus, the final decision of the CDS about the user under test (UUT) would be 'Unhealthy', as this state results in a higher reward than the 'Healthy' state. In this work, we termed this method of decision making as the Conflict-of-Opinions (CoOs) approach.

In summary, unlike a PAC-based CDS, the Executive of the proposed CDS uses multiple evidence generated from the model extracted by the Perceptor and applies multiple cognitive actions on the dynamic environment. The internal rewards generated in favor of every possible decision state give the PMAC-based CDS information to make a final decision by comparing among the rewards, giving the CDS self-awareness, self-consciousness about the dynamic environment, and independence from a defective dataset. The PMAC-based CDS thus has the ''conscience'' about the actions and non-reliability of the extracted model by the Perceptor. To generate multiple internal rewards, a CoO-based decision-making algorithm is applied in the Executive. In contrast, a PAC-based CDS uses the MAP rule for decision making based on a single internal award at each PAC, relying on the dataset and extracted model from the SL-based Perceptor. Therefore, in an intelligent healthcare screening process, the PMAC-based CDS is a more appropriate choice rather than a PAC-based because the SL cannot extract a converged reliable model from the defective dataset.

IV. PROPOSED ADMS USING CDS ARCHITECTURE AND ALGORITHMS

In this section, we describe the proposed CDS architecture and algorithm using a CoO-based decision-making approach for the screening process. The detailed architecture of the proposed CDS for health screening is shown in Fig. 5. Similar to the PAC-based CDS, a PMAC-based CDS has two main subsystems: (i) the Perceptor, and (ii) the Executive with a feedback channel linking them and it operates in three modes: (i) training, (ii) reasoning, and (iii) steady-state.

During the training mode, the data and information collected from the dataset will be converted to a 'model library' in the Perceptor and an 'action library' in the Executive. Also, the CDS in the training mode dynamically updates the knowledge in the Perceptor and the ''action-library'' in the Executive when the database is updated through the e-Health network. This update can be done in real-time in parallel to the reasoning mode, or during the steady-state mode.

The CDS will use the knowledge in the Perceptor ''model library'' for prediction of the health conditions of users with unknown health states. In the case when an anomaly in the user's health is detected or a request is placed by the user, the CDS can initiate the prediction mode. The trained CDS collects evidence about the user's health state and uses that information from the user to reason and predict the health state of the user, and then to determine whether any action is required based on a pre-defined set of policies and objectives. The policy can be, for example, a certain level of false alarm rate is acceptable in screening between the 'Healthy' and 'Unhealthy' states.

When the CDS makes a final decision based on current measurements, or there is no new request from the user, it goes into the steady-state mode. However, in specific

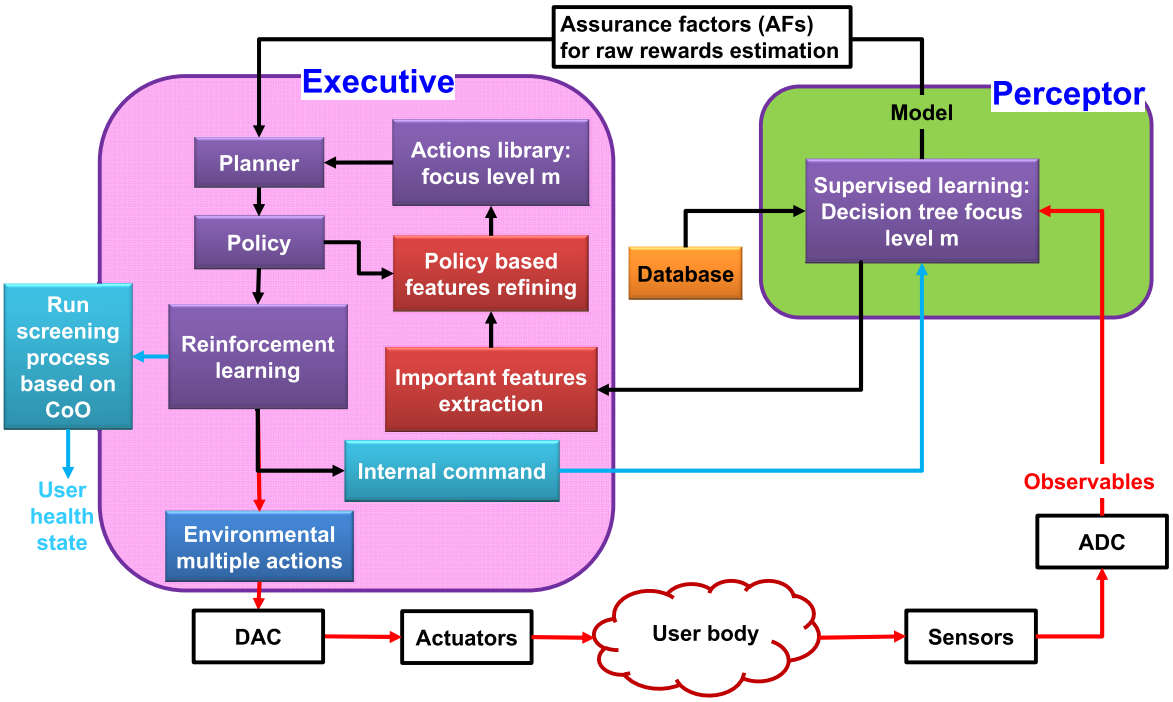

FIGURE 5. Block diagram of proposed CDS architecture for the ADMS of a smart e-Health home.

situations or upon receiving the user's request, the CDS will switch from steady-state to reasoning mode.

In brief, the following modes and functionalities constitute the proposed CDS as shown in Fig. 5.

I CDS training mode

a. Perceptor training mode.
b. Executive training mode.

II CDS reasoning mode

a. Feedback channel (multiple assurance factor calculation).
b. Executive (planner).
c. Executive (policy).
d. Executive (reinforcement learning and rewards calculation).
e. Executive (CoO-based CDM for screening process).

A. TRAINING MODE: PERCEPTOR AND EXECUTIVE

In a conventional CDS, the Perceptor uses *Bayesian filtering* based on the *Kalman filter* [16]. However, the *Kalman filter* cannot be used for non-Gaussian environments as the filter equations are extracted for a LGE [16]. Therefore, the Bayesian filter is not suitable for the proposed CDS. We exploited the decision tree to extract the posterior in CDS applied to NGNLE systems [10], [15]. This concept of posterior extraction using decision trees is extended in the proposed PMAC-based CDS. Extracting the posterior using decision trees is a common method in machine learning. The CDS training mode can be summarized in the following four parts:

a. Creating a jungle of decision-making trees.
b. Extracting the posterior
c. Extracting the knowledge- and action-space from the database
d. Action refinement in the Executive library based on a predefined policy.

Initially, when there exists no relevant model in a model library, the four-layered Bayesian modeling in the Perceptor extracts the statistical model of the system (see [10] for further details) using decision trees. The Bayesian modeling consists of four layers for an arbitrary focus level *m.* Here, in this paper, the decision tree level m is considered as the focus level m for the CDS.

1) LAYER I: NORMALIZATION

The extracted features from the measured physiological signals could have any value, and hence a large number of discretized cells are required for saving vacant spaces. For example, the output of the ECG signal can be represented as a set of features,

$$O = [feature(1), \ldots, feature(l), \ldots, feature(L)]. \quad (1)$$

where, L is number of extracted features from the dataset. Therefore, we normalize all extracted features as

$$\bar{O}(l) = \overline{feature}(l) = \frac{feature(l)}{\max\{abs(b^l_{\min}),\ abs(b^l_{\max})\}} \quad (2)$$

Here, $b^l_{\min}$ and $b^l_{\max}$ are the minimum and maximum value of the l_{th} feature. The data normalized in this way is sent to Layer II as the $\bar{O}$ for further processing. In this layer, the perceptor calculates L_m as the number of global nodes at focus level m, and $1 \leq m \leq M$ using permutation with repetition equation as:

$$L_m = \binom{L}{m} \tag{3}$$

For example, in Fig. 6 we have five extracted features in the dataset as [sex, age, height, breathing rate (BR), heart rate (HR)]. Therefore, using equation (3) at focus level 1, the number of global nodes is five. Similarly, number of new global nodes are 10 at focus level 2.

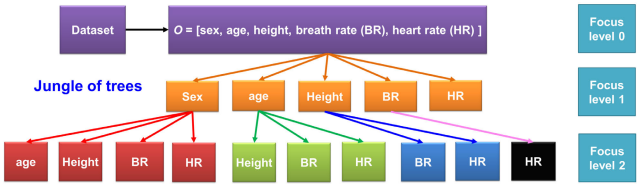

FIGURE 6. Example of global nodes of jungle of trees (here, 5 trees).

2) LAYER II: CREATING A JUNGLE OF TREES

In Layer II, the normalized values related to features are discretized with discretization steps Δx^k_i, and $1 \leq i \leq m$. Here, k is the PAC number and m is the current focus level. For simplicity, we define a *discretization factor* (DF^k_i) of features for focus level i as:

$$DF^k_i = 10\Delta x^k_i, \quad 1 \leq i \leq m \tag{4}$$

$$\mathbf{DF}^{k,m} = [DF^k_0, DF^k_1, \cdots, DF^k_i, \cdots, DF^k_m], \tag{5}$$

$$N^{k,i,l}_x = \frac{10(x^{k,i,l}_{\max} - x^{k,i,l}_{\min})}{DF^k_i}, \tag{6}$$

$$F^k_i = \sum_{l=1}^{L_i} N^{k,i,l}_x, \quad 1 \leq i \leq m, \; F^k_0 = 1. \tag{7}$$

Here, $N^{k,i,l}_x$ is the number of discretized cells in the x-axis for feature number $\hat{\mathrm{O}}^{k,i}_{DF}(l_i) = \overline{feature}(l_i, DF_i, i)$. Also, $x^{k,i,l}_{\min}$ and $x^{k,i,l}_{\max}$ are the minimum and maximum of the normalized feature ($abs(x^{k,i,l}_{\min}) \leq 1$, $abs(x^{k,i,l}_{\max}) \leq 1$).

Furthermore, F^k_i corresponds to the number of decision-trees branches (Eqs. (3) and (7)). For the desired complexity threshold, the CDS can update the current focus level m, $\mathbf{DF}^{k,m}$. Then, Layer II will send the discretized set of features $\hat{\boldsymbol{O}}^{k,m}_{DF}$ and $\mathbf{DF}^{k,m}$ to Layer III (Eqs. (2) and (8)).

$$\begin{aligned}
\hat{\boldsymbol{O}}^{k,m}_{DF} &= [\hat{O}^{k,m}_{\mathrm{DF}}, \hat{O}^{k,m-1}_{DF}, \ldots, \hat{O}^{k,i}_{DF}, \ldots, \hat{O}^{k,1}_{DF}], \\
\hat{O}^{k,i}_{DF} &= [\overline{feature}(1, DF_i, i), \ldots, \\
&\quad \overline{feature}(l_i, DF_i, i), \ldots, \\
&\quad \overline{feature}(L_i, DF_i, i)]. \\
\overline{O}^{k,m+1} &= [\overline{feature}(1, m+1), \ldots, \\
&\quad \overline{feature}(l_{m+1}, m+1), \ldots, \\
&\quad \overline{feature}(L_{m+1}, m+1)].
\end{aligned} \tag{8}$$

It should be noted that the required memory for saving models and action-space will increase as the number of focus levels increases in the CDS. Thus, to address the increasing algorithms complexity when the number of focus levels increase, we can define a bound for the maximum possible focus level as the *Complexity threshold*. Then, we can calculate the total acceptable branches of the decision tree as:

$$F^{total,k}_m = \prod_{f=2}^{m} F^k_i, \quad m \in \{1, 2, \ldots, M\}, \quad \text{and}$$
$$\text{and, } F^{total,k}_m \leq \textit{Complexity threshold}. \tag{9}$$

Furthermore, $F^{total,k}_m$ corresponds to the maximum number of tree branches at focus level m and perception action cycle k. For the desired predefined *Complexity threshold,* the CDS cannot increase the focus level more than M.

3) LAYER III: ESTIMATION OF PROBABILITIES AND DISCRETIZATION

In this layer, the system estimates the probability of a $\mathbf{HD}^k_n \in \{\text{“}Healthy\text{”}, \text{“}Unhealthy\text{”}\}$ for a given set of features, $\mathbf{O}^{k,m+1} = [O^{k,1}, O^{k,2}, \ldots, O^{k,i}, \ldots, O^{k,m}, O^{k,m+1}]$, i.e. $P(\mathbf{HD}^k_n|\mathbf{O}^{k,m+1})$. This is approximated as the probability of $\tilde{\mathbf{O}}^{k,m+1} = [\bar{\mathrm{O}}^{k,m+1}, \hat{\boldsymbol{O}}^{k,m}]$ (see eq. (8) and Fig. 7) for a given $\mathbf{HD}^k_n$, using the Monte-Carlo method and a jungle of decision trees as $P(\mathbf{HD}^k_n|\tilde{\mathbf{O}}^{k,m+1})$, where n is the discrete time. Therefore, the extracted posterior $P(\mathbf{HD}^k_n|\tilde{\mathbf{O}}^{k,m+1})$ can consider the correlations among $(m+1)$ features in each branch of tree in the jungle of trees. These estimated probabilities are saved in the Perceptor “model library” for future use. The Executive will use the extracted statistical probabilities for prediction by receiving them through the internal feedback channel to evaluate the actions virtually before applying them on the environment and creating the ‘action-library’.

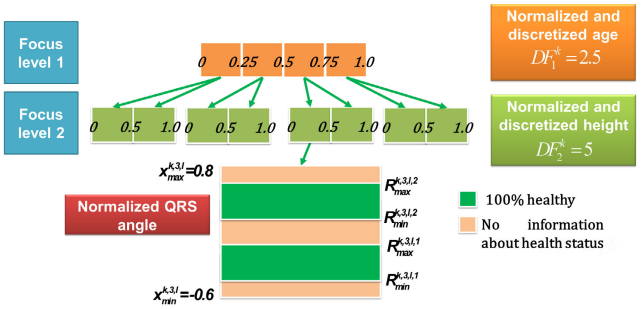

FIGURE 7. Example of decision boundaries extraction and action-library creation.

4) LAYER IV: CREATING ACTION-LIBRARY AND EXTRACTION OF EVIDENCE BOUNDARIES

In this layer, based on the applied system policy, the Executive estimates the decision boundaries and creates the

action-library. The action-library is the library of all possible actions the Executive can take for screening decision about the UUT. Here, we describe the process how the CDS finds the evidence that a UUT is healthy with an assurance of 100%. We use Eq. 10 to find the decision boundaries, which provide an assurance of 100% in favor of the 'Healthy' or 'Unhealthy' states (Fig. 7).

$$P(\mathbf{HD}_n^k | R_{\min}^{k,m+1,l,b} \leq \bar{\mathrm{O}}^{k,m+1}(l_{m+1}) \leq R_{\max}^{k,m+1,l,b}, \hat{\boldsymbol{O}}_{DF}^{k,m}) = 1 \tag{10}$$

Here, $b \in \{1, 2, \ldots, B_{m+1}^l\}$ and B_{m+1}^l are the total number of desired actions required for achieving a decision boundary containing evidence of 100% 'Healthy' state (or 'Unhealthy' state) at the focus level $(m+1)$, and branch l (see Fig. 7). The evidence boundaries of $R_{\min}^{k,m+1,l,b}$ and $R_{\max}^{k,m+1,l,b}$ will be saved in the model-library of the Perceptor.

In addition, the precision factor (PF) or the number of users within the decision boundaries (Healthy or Unhealthy) of the features are

$$\begin{aligned} PF_{b,m+1}^{k,l} &= U_{tot} \times P(R_{\min}^{k,m+1,l,b} \\ &\leq \bar{\mathrm{O}}^{k,m+1}(l_{m+1}) \leq R_{\max}^{k,m+1,l,b}, \hat{\boldsymbol{O}}_{DF}^{k,m}) \end{aligned} \tag{11}$$

Here, U_{tot} is total number of users in the training dataset. Therefore, $PF_{b,m+1}^{k,l}$ is the number of training patterns between $R_{\min}^{k,m+1,l,b}$ and $R_{\max}^{k,m+1,l,b}$ that are all 'Healthy' or 'Unhealthy'. The Executive keeps a record of $PF_{b,m+1}^{k,l}$, $[\hat{\mathrm{O}}_{DF}^{k,1}(l_1), \ldots, \hat{\mathrm{O}}_{DF}^{k,i}(l_i), \ldots, \hat{\mathrm{O}}_{DF}^{k,m}(l_m), \bar{\mathrm{O}}_{DF}^{k,m+1}(l_{m+1})]$ and information about the sensors required to extract the feature set of $[\hat{\mathrm{O}}_{DF}^{k,1}(l_1), \ldots, \hat{\mathrm{O}}_{DF}^{k,i}(l_i), \ldots, \hat{\mathrm{O}}_{DF}^{k,m}(l_m), \bar{\mathrm{O}}_{DF}^{k,m+1}(l_{m+1})]$ in the action-library. The action-space can be defined as follows:

$$C = \left\{ c_k \middle| c_k = \begin{array}{c} 1 - \textit{Actuating sensor} \\ (\textit{Healthy/Unhealthy evidence}) : \\ c^k(\tilde{\mathbf{O}}^{k,m+1}) \\ 1.1 - \textit{Time domain features} \\ 1.2 - \textit{Frequency doman features} \\ 1.3 - \textit{Statistical features} \\ 5 - \textit{Internal commands} : \\ \textit{Increase } m, \ (m+1) < M \end{array} \right\}. \tag{12}$$

Also, all decision boundaries for action space can be shown as:

$$R_{\textit{healthy or unhealthy}} = \left\{ r_k^{m,l,b} \textit{for } c_k \middle| \begin{array}{c} r_k^{m,l,b} = [R_{\min}^{k,m+1,l,b}, R_{\min}^{k,m+1,l,b}], \\ PF_{b,m+1}^{k,l}(r_k^{m,l,b}). \end{array} \right\}. \tag{13}$$

Here, c_k is the action at the k_{th} PAC and m is the focus level. The action-space contains information about all possible actions that the Executive can perform during the reasoning mode to provide evidence in favor of 'Healthy' or 'Unhealthy' state. Using the complexity threshold defined in eq. (9). Using eqs. (14)-(16), we can obtain the number of training users in each branch of decision trees:

$$\begin{aligned} U_{m+1}^{k,l} &= U_{tot} \times P(x_{\min}^{k,m+1,l} \leq \bar{\mathrm{O}}^{k,m+1}(l_{m+1}) \\ &\leq x_{\max}^{k,m+1,l}, \hat{\boldsymbol{O}}_{DF}^{k,m}) \end{aligned} \tag{14}$$

$$U_{m+1}^{k,l} \geq U_{\min}, \tag{15}$$

$$U_{\min} = \frac{5}{Threshold_{DE}}. \tag{16}$$

Here, $U_{m+1}^{k,l}$ is number of training data in branch l of the decision tree and focus level $(m+1)$. Also, in eq. (16), $U_{\min}$ is the minimum required number of users for the l_{th} branch and focus level $(m+1)$ to enable extraction of a reliable model. In eq. (15), the $Threshold_{DE}$ is a predefined desired diagnostic error. Then, the information related to the extracted decision trees is saved in the memories of the Perceptor and Executive.

The procedure for finding an evidence of 100% assurance that the UUT is "Unhealthy" follows a similar approach.

B. REASONING MODE: CALCULATING RAW INTERNAL REWARDS IN FEEDBACK CHANNEL

As mentioned earlier, unlike the typical RL, the internal reward gives the CDS self-awareness, self-consciousness about the dynamic environment, and independence from a defective dataset. In this section, we explain a simple approach to estimate the possible error using the fuzzy nature of the assurance factor concept [10].

Fuzzy logic means that the "logic" values of a variable can be a real number between 0 and 1 [46]–[48]. Also, fuzzy logic is widely used for medical decision making in health environments such as Value-Laden choices [49], medical decision making in the intensive care unit (ICU) [50], and atrial fibrillation detection [51], [52]. Also, the fuzzy nature of the PAC process in CDS was described in [10]. Fuzzy logic can be used as the assurance prior to making a decision. For example, a person or machine can make a wrong decision when the assurance is less than 1. Similarly, the proposed CDS measures the assurance of a decision between 0 and 1 after taking actions on the environment.

The estimation process of internal reward (or diagnosis error) for the proposed CDS can be explained with the help of Fig. 8. The estimation process of false alarm follows a similar approach. As mentioned earlier, the initial decision of the CDS about the UUT (U_{test}) is 'Unhealthy'. The CDS performs some actions on the environment and uses the CoO

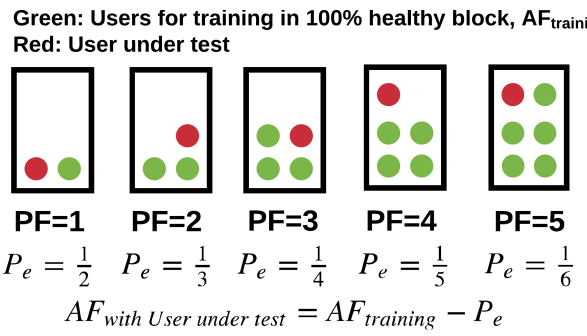

FIGURE 8. Example for diagnosis error (DE) and false alarm (FA) estimation. The precision factor (PF) is introduced for each case.

to reach a final decision. Once the CDS finds stronger evidence in favor of the ''Healthy'' state than the ''Unhealthy'' state, it changes the decision to 'Healthy'. For example, in the case of $PF = 4$, there are 4 healthy users from the training dataset whose data remain with a range of r, i.e. within the range r, all 4 users from the training dataset are healthy. Now if the data of the UUT falls within the range r, the conditional probability error (estimated diagnosis error) for a decision of ''Healthy'' would be 0.2 (see Fig. 7).

In general, we can define the AF for the UUT as 'Healthy' using, (defining the AF for the UUT as 'Unhealthy' follows similar procedure)

$$\begin{aligned} P(U_{test} &= Healthy| \\ R^{k,m+1,l,b}_{\min,Healthy} &\le \bar{O}^{k,m+1}_{U_{test}}(l_{m+1}) \le R^{k,m+1,l,b}_{\max,Healthy}, \hat{\boldsymbol{O}}^{k,m}_{DF,U_{test}}) \\ &= \frac{PF^{k,l,Healthy}_{b,m+1}}{PF^{k,l,Healthy}_{b,m+1}+1}, \end{aligned} \tag{17}$$

$$AF^{k}_{DE} = \frac{PF^{k,l,Healthy}_{b,m+1}}{PF^{k,l,Healthy}_{b,m+1}+1}. \tag{18}$$

Here, AF^{k}_{DE} is the assurance factor in favor of the 'Healthy' state and DE stands for the estimated diagnosis error. Similar to AF^{k}_{DE}, the assurance factor for false alarm, AF^{k}_{FA} can be estimated at k th PAC as

$$\begin{aligned} P(U_{test} &= Unhealthy| \\ R^{k,m+1,l,b}_{\min,Unhealthy} &\le \bar{O}^{k,m+1}_{U_{test}}(l_{m+1}) \le R^{k,m+1,l,b}_{\max,Unhealthy}, \hat{\boldsymbol{O}}^{k,m}_{DF,U_{test}}) \\ &= \frac{PF^{k,l,Unhealthy}_{b,m+1}}{PF^{k,l,Unhealthy}_{b,m+1}+1}, \end{aligned} \tag{19}$$

$$AF^{k}_{FA} = \frac{PF^{k,l,Unhealthy}_{b,m+1}}{PF^{k,l,Unhealthy}_{b,m+1}+1}. \tag{20}$$

C. REASONING MODE: PERCEPTOR AND SIMPLE EXECUTIVE

The CDS initiates the reasoning mode when an anomaly in the user's health is detected or a request is placed by the user. The trained CDS gathers evidence about the user's health state and uses that information to reason and predict the health state of the user. The CDS then determines whether any action is required based on a pre-defined set of policies and objectives.

The Executive is an essential part of any CDS. It is responsible for improving the decision-making accuracy by applying action on the NGNLHE. For example, the Executive can activate the actuators in the smart home or send the internal commands to the Perceptor for changing the modeling configurations such as $\mathbf{DF}^{k,m}$. The Executive provides non-monotonic reasoning to the CDS by using the internal reward and changing its focus level. The Executive designed in this work includes three parts (see Fig. 5): planner including the action-library, policy, and learning using a cost-to-go function [10]–[15].

Algorithm 1 Conflict of Opinions (CoOs)

CDS initial decision: UUT is Unhealthy
if $T_{Healthy} = 0$ **then**
  Keep decision to Unhealthy.
  Stop process and turn on steady state.
elseif $T_{Unhealthy} = 0$ **then**
  Keep decision as Unhealthy.
  Stop process and turn on steady state.
elseif $k \le T_{Unhealthy} \& k \le T_{Healthy}$ **then**
  if $(k \times (1 - rw^{k}_{DE}))^{w_{DE}} > (k \times (1 - rw^{k}_{FA}))^{w_{FA}}$ **then**
    Change decision to Healthy.
    else
      Keep/change decision as Unhealthy.
    end of if
elseif $k > T_{Unhealthy} \& k \le T_{Healthy}$ **then**
    if $(k \times (1 - rw^{k}_{DE})^{w_{DE}} > T_{Unhealthy} \times (1 - rw^{k}_{FA}))^{w_{FA}}$ **then**
      Change decision to ''Healthy''.
      Stop process and turn on steady state.
    else
      Keep/change decision as Unhealthy.
    end of if
elseif $k \le T_{Unhealthy} \& k > T_{Healthy}$ **then**
    if $(T_{Healthy} \times (1 - rw^{k}_{DE}))^{w_{DE}} > (k \times (1 - rw^{k}_{FA}))^{w_{FA}}$ **then**
      Change decision to ''Healthy''.
    else
      Keep/change decision as Unhealthy.
      Stop process and turn on steady state.
    end of if
else
    if $(T_{Healthy} \times (1 - rw^{k}_{DE}))^{w_{DE}} > (T_{Unhealthy} \times (1 - rw^{k}_{FA}))^{w_{FA}}$ **then**
      Change decision to Healthy.
      Stop process and turn on steady state.
  else
      Keep/change decision as Unhealthy.
      Stop process and turn on steady state.
  end of if
end of if

1) PLANNER AND POLICY

In a CDS, the policy is defined as the desired goals that the CDS attempts to achieve in each PAC during the screening process. Here, the goal is to achieve a pre-defined $Threshold_{DE}$ of diagnosis error (DE) by minimizing the false alarm (FA) rates. Then, based on the $Threshold_{DE}$, the actions for providing evidence in favor of 100% healthy state in the action-space can be refined by the planner as:

$$PF^{k,l}_{b,m+1,Healthy} \ge PF^{k,l,\min}_{b,m+1,Healthy} = \frac{1}{Threshold_{DE}} - 1. \tag{21}$$

For example, if the predefined desired diagnosis error threshold is 10% at focus level 3, then the number of training

patterns within the range with 100% "Healthy" states should be $PF^{k,l}_{b,3,healthy} \geq PF^{k,l,\min}_{b,3,healthy} \geq 9$. Then, the acceptable actions that can give evidence in favor of 100% 'Unhealthy' state can be refined by the planner using eqs. (22) and (23).

$$PF^{k,l}_{b,m+1,Unhealthy} \geq PF^{k,l,\min}_{b,m+1,Unhealthy}, \tag{22}$$

$$PF^{k,l,\min}_{b,m+1,Unhealthy} = floor\left(\frac{P(U_{test} = Unhealthy)}{P(U_{test} = Healthy)} \times PF^{k,l,\min}_{b,m+1,Healthy}\right)$$

$$if \;\; PF^{k,l,\min}_{b,m+1,Unhealthy} < 1 \Rightarrow PF^{k,l,\min}_{b,m+1,Unhealthy} = 1 \tag{23}$$

The reason behind multiplying $PF^{k,l,\min}_{b,m+1,Healthy}$ with the ratio of 'Unhealthy' prior, $P(U_{test} = Unhealthy)$ to the 'Healthy' prior $P(U_{test} = Healthy)$ in Eq. 23 can be explained by an example. Let us assume a dataset where there are 1000 'Healthy' and 100 'Unhealthy' training patterns. Therefore, because the prevalence of healthy training patterns are more than unhealthy training patterns, it more likely to find a subset of at least 50 'Healthy' persons, whose data remain within a certain range ($PF^{k,l,min}_{b,m+1,Healthy} = 50$) than to find such a subset of 50 'Unhealthy' persons. In such a case, the CDS uses eq. 23 and finds a subset with at least 5 'Unhealthy' persons, whose data remain within a certain range. Therefore, the Bayesian statistics inspired by Eq. 23 represents a better approach of applying the desired predefined policy to refine actions by the planner.

2) ERROR CALCULATION AND CoO-BASED DECISION MAKING

The assurance factor (AF) measures the expected assurance about the decision after the current action c_k. Therefore, multiple final rewards for the estimation of false alarm (FA) and diagnosis error (DE) can be calculated as:

$$rw^k_{FA} = \begin{cases} 1 - \frac{\sum_{t=1}^{k} AF^t_{FA}}{k} & k \leq T_{Unhealthy} \\ rw^{T_{Unhealthy}}_{FA} & k > T_{Unhealthy} \end{cases} \tag{24}$$

$$rw^k_{DE} = \begin{cases} 1 - \frac{\sum_{t=1}^{k} AF^t_{DE}}{k} & k \leq T_{Healthy} \\ rw^{T_{Healthy}}_{DE} & k > T_{Healthy} \end{cases} \tag{25}$$

Here, $T_{Unhealthy}$ and $T_{Healthy}$ are the maximum number of actions available in the action-space to provide evidence of 100% 'Unhealthy' and 100% 'Healthy' states, respectively. Also, rw^k_{FA} and rw^k_{DE} is the estimated false alarm and the estimated diagnosis error for the UUT, respectively. The process of CoO uses the estimated rewards in eqs. (24) and (25) that are presented in Algorithm 2.

For the screening process, the initial decision of the CDS about the UUT at the beginning of the PMAC ($k = 0$) is 'Unhealthy'. For a specific UUT or based on the pre-defined policy, if there exists no such action in the action-space that can provide 100% evidence that the UUT is 'Healthy', the Executive does not change its initial decision and moves to the steady-state with a final decision of 'Unhealthy' about

Algorithm 2 CDS for User-Health Prediction (planner, Reinforcement Learning and Policy in Executive, Running Diagnostic Test in the Perceptor)

Input: The observables and features from the database for each user for the focus level m, models, ranges, policy (screening process, desired diagnosis error, $w_{DE}, w_{FA}, \ldots$), a database of users

Output: Decision about the health state of the UUT

Initialization:
$c_0 \leftarrow$ The actions, [Vital signs and portable sensors, $\cdots$] apply on the user
Start advanced actions such as 12 leads ECG or ... if c_0 shows an anomaly in the user's health or a request is placed by the user.
Load the model at focus level $m = 0$ and action-space C, Decision = 0 (UUT unhealthy), $Threshold_{DE}$.
$c_{k=0} \leftarrow$ an action randomly selected from C and focus level 0
Apply to $c_{k=0}$ to UUT
Extract features $\tilde{\mathbf{O}}^{k=0,1}$ and choose one of them with maximum $PF^{k=0,l}_{b,1}$, load $r^{m=0,l,b}_{k=0}$
Calculate $rw^{k=0}_{DE}$ and $rw^{k=0}_{FA}$

while $k \leq (K-1)$ **then**
  Update features based on

1) **Planning**
  $\boldsymbol{C\_buf} \leftarrow C(m)$

Learning
  for all actions ($s \in \boldsymbol{C\_buf}$) **do**
    for $l = 1$ to L_m **do**
      for $b = 1$ to B^l_{m+1}
        Calculate $rw^{k+1,s}_{DE}$
        Calculate $rw^{k+1,s}_{FA}$
        Calculate $f^{(k+1)}_s(rw^{k+1,s}_{DE}, rw^{k+1,s}_{FA})$
      End for
    End for
  End for
  Extract S', L' *and* B'
  Remove S' from $\boldsymbol{C\_buf}$
  if $S' < 1$ **then**
    Calculate $F^{total,\,k}_{m+1}$
    if $F^{total,\,k}_{m+1} \leq$ *Complexity threshold* **then**
      Increase focus level m by 1 (if $U_{\min}$ met)
      $k \leftarrow k+1$
    else
      Message: Not meeting $Threshold_{DE}$
      Decision = Unhealthy
      Return Decision
    end if
  else
    Apply action (sensor activation) S' on user ($c^{S'}_{k+1}$)
    $k \leftarrow k+1$

Run screening process
  $O_{U_{test}} \leftarrow$ *Extracted features of* $c^{S'}_{k+1}$

Algorithm 2 *(Continued.)* CDS for User-Health Prediction (planner, Rein- forcement Learning and Policy in Executive, Running Diag- nostic Test in the Perceptor)

29: **if** $R_{\min}^{k,m+1,L',B'} \leq \bar{O}_{U_{test}}^{k,m+1}(L') \leq R_{\max}^{k,m+1,L',B'}$ and $\hat{O}_{DF,U_{test}}^{k,m}$ **then**
30: Calculate rw_{DE}^{k}
31: Calculate rw_{FA}^{k}
32: Run Algorithm 1 for CoO Decision making
33: **End while**

the UUT. If the CDS finds 100% evidence of the UUT being 'Healthy' but does not find 100% evidence of the user being 'Unhealthy', the CDS changes the final to decision to 'Healthy' and moves to the steady-state. However, in the case when the CDS finds 100% evidence for the UUT in favor of both the 'Healthy' and 'Unhealthy' states, then the CDS checks whether the eq. (26) is satisfied at kth PMAC (Details are provided in Algorithm 2):

$$(k \times (1 - rw_{DE}^{k}))^{w_{DE}} > (k \times (1 - rw_{FA}^{k}))^{w_{FA}} \tag{26}$$

Here, w_{DE} and w_{FA} are arbitrary pre-defined weights associated with the diagnosis error and the false alarm, respectively, and are determined based on the trade-off between them.

3) LEARNING USING PREDICTION

a: EXECUTIVE ACTIONS

The purpose of the Executive is to find prospective actions that can optimize the cost-to-go function. Then, the system will apply some relevant actions on the NGNLHE based on the actions required for finding 100% evidence in favor of 'Healthy' or 'Unhealthy' states. Here, relevant actions can be, for example, asking for related information to the user or activating sensors for new measurements. For each health condition, the Executive activates the sensors to obtain maximum information about the health conditions using the planning and learning sections. Reinforcement learning will be done once the database is updated with new information or the smart e-Health system is upgraded with new sensors. The data obtained from the Executive through reinforcement learning can also be updated with new measurements from the sensors at a later time.

The false alarm and diagnosis error due to the virtual environmental action of c_{k+1}^{s} can be predicted by,

$$rw_{FA}^{k+1,s} = \begin{cases} 1 - \frac{\sum_{t=1}^{k} AF_{FA}^{t} + AF_{FA}^{k+1,s}}{k+1} & (k+1) \leq T_{Unhealthy} \\ rw_{FA}^{T_{Unhealthy}} & (k+1) > T_{Unhealthy} \end{cases}, \tag{27}$$

$$rw_{DE}^{k+1,s} = \begin{cases} 1 - \frac{\sum_{t=1}^{k} AF_{DE}^{t} + AF_{DE}^{k+1,s}}{k+1} & k+1 \leq T_{Healthy} \\ rw_{DE}^{T_{Healthy}} & k+1 > T_{Healthy} \end{cases}, \tag{28}$$

$$AF_{FA}^{k+1,s} = \frac{PF_{b,m+1,Unhealthy}^{k+1,l,s}}{PF_{b,m+1,Unhealthy}^{k+1,l,s} + 1}. \tag{29}$$

$$AF_{DE}^{k+1,s} = \frac{PF_{b,m+1,Healthy}^{k+1,l,s}}{PF_{b,m+1,Healthy}^{k+1,l,s} + 1}. \tag{30}$$

Here, $s \in \{1, 2, \ldots, S\}$ and S is the total number of desired actions that can be applied for the screening process. Also, in eqs. (29) and (30), $PF_{b,m+1,Healthy}^{k+1,l,s}$ and $PF_{b,m+1,Unhealthy}^{k+1,l,s}$ are the precision factors received through the internal feedback from the Perceptor corresponding to the 'Healthy' and 'Unhealthy' states, respectively. Then, the cost-to-go function for the desired action c_{k+1}^{s} can be calculated using eq. (31) as,

$$f_s^{(k+1)}(rw_{DE}^{k+1,s}, rw_{FA}^{k+1,s}) = \begin{cases} \frac{(rw_{DE}^{k+1,s} - rw_{DE}^{k})^{wDE}}{(rw_{FA}^{k+1,s} - rw_{FA}^{k})^{wFA}}, & s \in \{1, 2, \ldots, S\} \\ f^{k}(rw_{DE}^{k}, rw_{FA}^{k}) & s = 0 \end{cases}, \tag{31}$$

$$(feature\_location)_s^{(k+1)} = [l, b]. \tag{32}$$

Therefore, we can find the action $c_{k+1}^{S'}$ that minimizes the cost-to-go function as,

$$S' = \underset{S \in \{0,1,2,3,\ldots,S\}}{\operatorname{argmin}} (f_s^{k+1}). \quad [L', B'] = f_{s'}^{k+1}. \tag{33}$$

As a result, the actions to be applied on the environment can be selected as,

$$c_{k+1} = c_{k+1}^{S'}, \quad for\ S' \geq 1. \tag{34}$$

Therefore, c_{k+1} is the best action to be applied on the environment to improve the CoO-based decision-making performance based on the desired policy set by the user. Algorithm 2 shows the outline of the main processes of the global PAC of the proposed CDS.

V. CASE STUDY: SCREENING OF A USER WITH OR WITHOUT ARRHYTHMIA

Cardiovascular disease (CVD) is among the leading causes of death in the world [53]. Arrhythmia or irregular heartbeat is the most common CVD in persons older than 35 years with millions of people in the world having some forms of Arrhythmia [54], [57]. In the USA, 850,000 persons are hospitalized each year due to Arrhythmia [54]. In addition, about 326,000 out-of-hospital sudden cardiac arrests (OHSCA) can happen in the USA every year with a survival rate of 10-11% [54] and more than 80% of sudden cardiac death results from ventricular Arrhythmia [55], [56]. However, the survival rate in the case of OHSCA can be improved to 33% if it occurs in front of another person(s) [55] which makes early identification of arrhythmia critical. It was found that 16-17% of Canadians are not aware of having an Arrhythmia [58], making them vulnerable to potential fatal consequences. Therefore, continuous monitoring for and early identification of arrhythmia is of paramount significance to avoid potentially fatal consequences.

In clinical settings, Arrhythmia is generally diagnosed by the 12-leads ECG [59] or by the Holter monitor [60]. However, these methods can only diagnose about 50% of Arrhythmia [61]. Also, portable single-lead ECG devices are gaining popularity as a tool for continuous, in-home monitoring of cardiovascular activity.

We used the proposed CDS to distinguish between 'Arrythmia' and 'Normal' ECG as a proof-of-concept application of CDS for health screening in presence of a defective dataset. Here, we chose a dataset of single-lead ECGs posted in PhysioNet Computing in Cardiology Challenge (CINC) 2017 [62] to implement the proposed algorithm.

The CINC 2017 dataset can be considered as an example of defective dataset, because all submitted trained models have problems of overfitting, resulting the performance of the models to drop significantly in the testing phases [62]. It was mentioned in [63] that estimation of the health state using the CINC 2017 database is a non-trivial problem. In addition, the examiners concluded that the number of training patterns in the CINC 2017 dataset are not enough to provide advantage for complicated algorithms over simple algorithms (Defective database) [63]. It is also mentioned in [63] that more training patterns and better labeling of CINC 2017 dataset are required for better performance. Although, the defective CINC 2017 dataset may not be reliable for accurate arrhythmia diagnostic test, it may still be useful for primary screening [63]. Figure 9 shows the extracted Heart rate (HR) using an available MATLAB program from the Physionet website for CINC 2017 database [64] and the HR in clinically valid MATLAB (UCI) dataset. The details about the MATLAB dataset are provided in [10]. The MATLAB dataset contains newborn to elderly people. However, in the CINC 2017 database, age and sex are not provided. Figure 9 shows that normal HR should be between 55-101 Beats/min based on MATLAB dataset [10]. Thus, HR lower than 55 Beat/min is called Bradycardia or slow HR and HR higher than 101 Beat/min is called Tachycardia or fast HR. Both Bradycardia and Tachycardia are two well-known Arrhythmia classes. Figure 9 shows that 1371 out of 5076 (∼27% of normal rhythms) are out of normal HR range and this misleads any ML-based AI approach that trusts the dataset and labeling. Therefore, we selected CINC 2017 as the defective dataset to implement a proof-of-concept case study of the proposed PMAC-based CDS.

The provided ECG recordings in the CINC 2017 database are collected using a US Food and Drug Administration (FDA) approved single-lead portable ECG device, KardiaMobile from AliveCor [62]. The database contains 8,528 single-lead ECG recordings from 9 s to just over 60 s collected at a sampling rate of 300 Hz. Table 1 shows the number of ECG waveforms in each of the four classes. However, we used this dataset to screen between two binary classes of healthy (normal rhythms) and unhealthy (AF and other rhythms and noisy recordings) states as a proof-of-concept application of our proposed CDS.

TABLE 1. Prevalence in CINC 2017 database (priors).

Class	Users out of 8528 persons	Prevalence %
Normal rhythms	5076	59.5
Atrial fibrillation	758	8.9
Other rhythms	2415	28.3
Noisy recordings	279	3.3

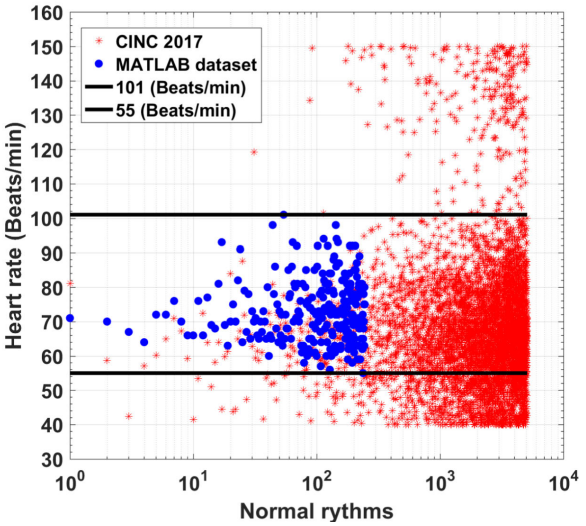

FIGURE 9. Heart rate of persons labeled as normal rhythms in CINC2017 [51] and MATLAB dataset [10].

A. SIMULATION PARAMETERS AND CoO DECISION MAKING EXAMPLE FOR CASE STUDY

Here, we used a validation dataset from [51], [52] and removed them from the training dataset to verify the performance of the proposed CDS. Detailed information related to training dataset and validation dataset can be found in [62]. The simulation parameters used for the CDS-based screening process are presented in Table 2. We extracted the features using the available MATLAB program from the Physionet website [64]. The program extracts 188 features from each ECG signal [64]. For simplicity, the CDS uses only feature 80 as the node at focus level 1, while at focus level 2,

TABLE 2. Simulation parameters of CDS.

Simulation parameters	Value
Focus level m	3
Feature in $i = 1$	1 (feature 80)
Feature in $i = 2$	187
$DF^k_{i=1}$	5
$DF^k_{i=2}$	5
Normalization range	|feature value| ≤1
w_{DE}	1
w_{FA}	1

TABLE 3. Summary of simulation results for proposed CDS.

Policy Diagnosis error (DE)	Final Real DE %	Final average Internal rewards: DE %	Final Real False alarm (FA) %	Final average Internal rewards: FA %	% of the UUTs resolved by CoO	$PF_{b,3}^{k,l,\min}$ Healthy	$PF_{b,3}^{k,l,\min}$ Unhealthy
DE≤25%	13.2	8	20.1	22	99.3	3	2
DE≤10%	9.9	6.5	25	35	98.3	9	6
DE≤5.9%	6.6	5.8	28.4	47	83.3	16	11
DE≤2.5%	4.6	2.8	54.7	42	11.7	39	26

the remaining 187 features are used (see Sections 4.A.1-4.A.4, Figs. 6 and 7). At focus level 3, the CDS extracts important features from the measured ECG signals that carry information corresponding to the healthy or unhealthy state of the UUT. Also, all features are normalized to their absolute maximum value at focus level 0 (see Table 2).

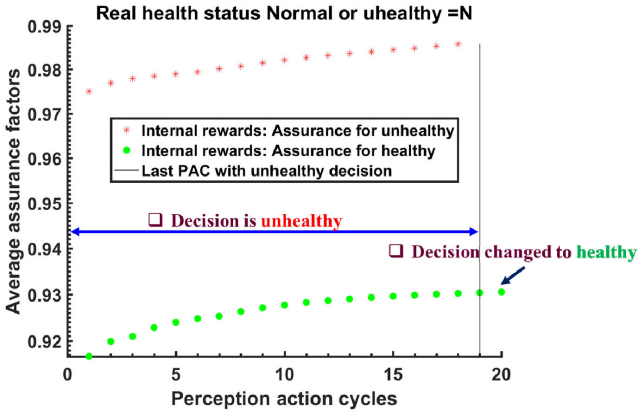

FIGURE 10. Example of decision-making based on conflict of opinions (CoO) ($PF_{b,3}^{k,l,\min}(Healthy) = 3$, $PF_{b,3}^{k,l,\min}(Unhealthy) = 2$, N: Normal rhythm/Healthy).

Figure 10 shows an example of the CoO-inspired decision-making process. The UUT in this example had an ECG with 'Normal rhythm', and was therefore, considered to be in a 'Healthy' state. As shown in Fig. 10, the decision about the UUT's health state is 'Unhealthy' in all PACs from 0 to 19. However, the CDS changes the decision to "Healthy" in PAC 20 through non-monotonic reasoning i.e. the earlier decision was invalidated by adding new evidence. The CDS stays on the decision of "Healthy" based on the current measurement from the sensor as 1) there remains no more evidence showing that the person is "Unhealthy" and 2) the weight of the evidence in favor of a 'Healthy' state is higher (See section 4.C.2, Eq. (26) and Algorithm 1). However, if the CDS finds new evidence in favor of the "Unhealthy" state in future measurements, it may change the decision to "Unhealthy".

B. AVERAGE ESTIMATED AND REAL LEARNING CURVES FOR CASE STUDY FOR DIFFERENT PREDEFINED POLICIES

We simulate the CDS for four predefined goals and policies. The objective of the CDS is to minimize the false alarm at four different levels of desired diagnosis errors, *i.e.* 25%, 10%, 5.9% and 2.5% (see section 4.C.1, $Threshold_{DE}$). The simulation parameters and a summary of the results are presented in Table 3. The simulation results of average internal rewards for false alarm and diagnosis error estimation (see section 4.C.2 and Eqs. (24) and (25)) as well as the real false alarm and diagnosis error are shown in Fig. 11 (a)-(d) with respect to the PAC number for the desired policy of diagnosis error ($Threshold_{DE}$) less than 25%, 10%, 5.9% and 2.5%, respectively. It can be seen from Figs. 11(a)-(d) that the CDS-generated average internal rewards for diagnosis error and false alarm reach to a good agreement at higher PMAC with the actual average diagnosis error and average false alarm (see Table 3, also).

It can be seen from Figs. 11 (a)-(b) and Table 3 that the CDS can fulfill the requested policies. However, in Figs. 11 (c) and (d) (see Table 3 also), the final diagnosis errors are a little higher than the desired values. This is mainly because when the policy changes from the required DE of 5.9% to 2.5%, the number of UUTs who were successfully resolved by CoO decreased from 83.3% and 11.7% (see Table 3). That is, the proposed CDS cannot meet the required diagnosis errors when the number of users for CoO decrease significantly (see Table 3).

In Fig. 11 (a), both the estimated and real diagnosis error are high at the beginning. This is because actions used at the beginning cause some actual 'Unhealthy' UUTs to be falsely diagnosed as 'Healthy'. However, as the number of PMACs increases and the CDS finds new evidence at every PMAC, it can change the decision about them (See Fig. 10 also). For a similar reason, the average estimated diagnosis error in Fig. 11 (b) is initially high, but showed a good agreement with the real average diagnosis error at higher PMAC numbers. In addition, the number of PMACs decreased from Fig.11 (a) to Fig. 11 (d). This is due to the fact that 1) the number of users with both actions decreases (Figs. 11 (c)-(d)); and 2) based on the policies applied (Figs. 11 (b)-(d)), and less actions are now available in the action-space (see section 4.C.1 and Eqs. (21)-(23)).

Like the diagnosis error, estimation of the false alarm by the CDS also depends on the number of available users with both available actions. The CDS performs the screening process by minimizing the false alarm for a predefined desired diagnosis error. It can be seen in Fig.11 (a) that there is a good agreement between the final estimated false alarm and real false alarm. Also, the final real false alarms are lower than

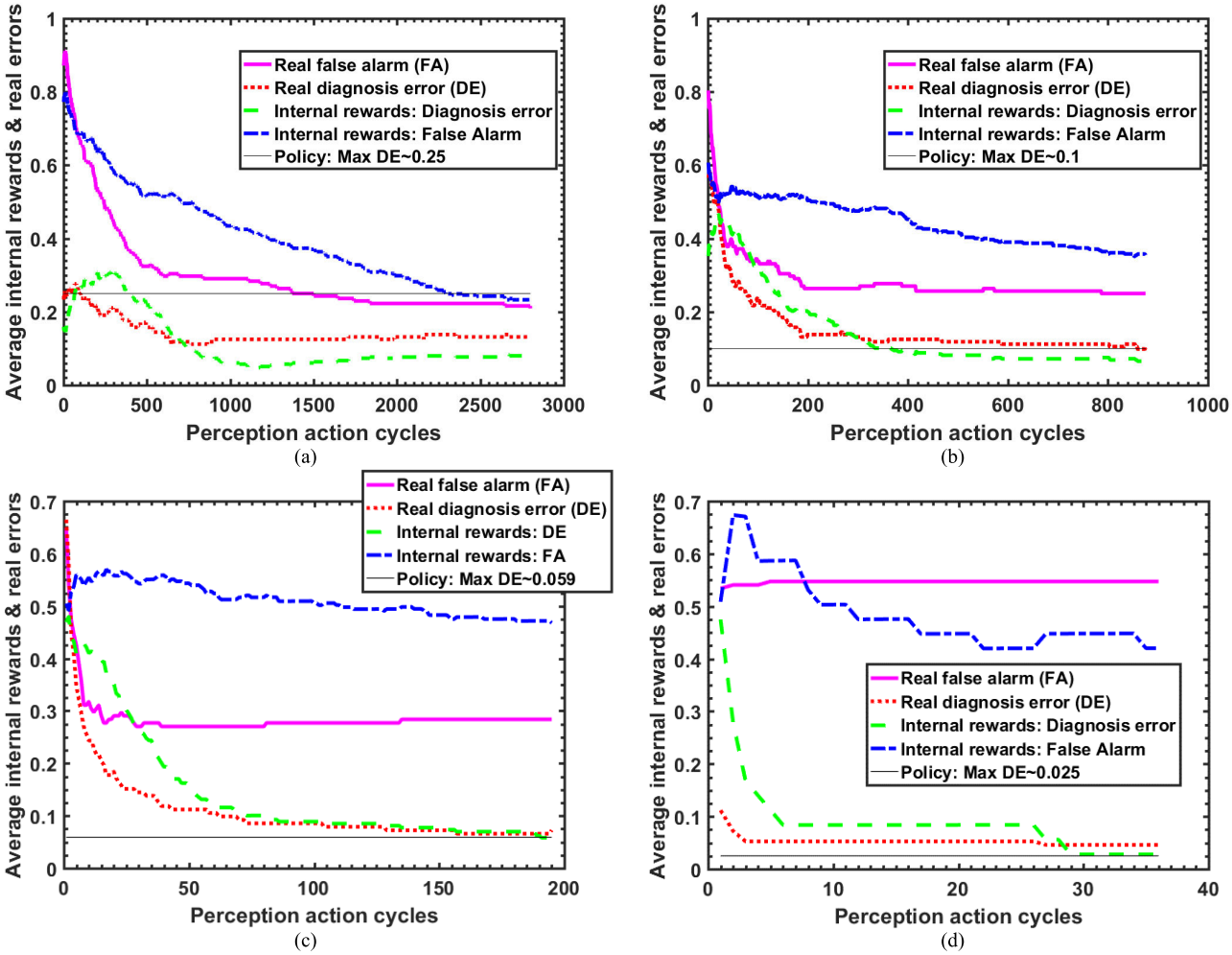

FIGURE 11. Average internal rewards vs. average real diagnosis error and false alarm, for desired diagnosis error (DE) (a) DE≤25%, (b) DE≤10%, (c) DE≤5.9%, and (d) DE≤2.5%.

the CDS-estimated false alarms (Fig.11 (a)-(c)). However, in Fig. 11(d), the estimated false alarm is lower than the actual false alarm, which results from the fact that the estimation was done based on ∼11.7% of the users (see Table 3). Also, unlike the estimated false alarm rates in Fig. 11 (a)-(b), it can be seen in Fig. 11 (c) that the estimated false alarm is high for the earlier PMACs, while real false alarm decreased. This is mainly because when the policy changes to the required DE of 5.9%, the number of UUTs who were successfully resolved by CoO also decreased to 83.3%. The remaining 16.7% UUTs contribute to the inaccurate estimation of the real false alarm in earlier PMACs.

In general, based on Table 3, the average final diagnosis error decreased from 13.2% in Fig. 11 (a) to 9.9% in Fig. 11 (b), 6.6% in Fig. 11 (c) and 4.6% in Fig. 11 (d). However, the trade-off of decreasing average final diagnosis error is the increment of the average final false alarm from 20.1% in Fig. 11(a) to 25% in Fig. 11(b), 28.4% in Fig. 11(c) and 57% in Fig. 11(d). It can be seen from Fig.11 (c) and Fig. 11 (d) that the trade-off of 2% improvement of average final diagnosis error is a 28.6% increase in the average final false alarm. This can be attributed to the fact that the proposed CDS can apply CoO only on 12% of users in this policy in Fig. 11(d) (see Table 3 also). As a consequence, for improving diagnosis error more than 5.9% a significant penalty for false alarm increment is paid.

In summary, we can conclude that the CDS should have more than 80% (ideally, 98%) UUTs with CoO (For example Fig. 11(a)-(c), see Table 3 also). The percentage of decisions made by the CoO out of the total decisions can be used as another internal metric and reward for the proposed CDS. This metric would give the proposed CDS a 'self-awareness' about the reliability of its performance.

VI. CONCLUSION

In recent years, there has been a growing interest in developing smart interactive cyber-physical systems (CPS) such as smart home and e-Health. An autonomic decision-making system (ADMS) is of paramount importance for the autonomic computing layer of such systems. The ADMS for

a smart e-Health Home may include functionalities such as real-time dynamic training or decision-making, screening process, treatment, healing tracking as well as recommendations for healthy living. In this paper, we proposed a PMAC-based cognitive dynamic system (CDS) for an ADMS to enable automatic screening of human health with an acceptable level of false alarm rates. We also proposed a CoO-inspired decision-making algorithm that allows the proposed CDS to make a decision at a pre-defined level of confidence even when the training dataset itself is poorly labeled or unbalanced.

The system architecture and algorithms are developed to realize a health screening (i.e., healthy or unhealthy) application with an acceptable level of the false alarm policy. To illustrate the application of the proposed system, a proof-of-concept case study is performed on a defective dataset of ECG traces. The performance of the proposed CDS shows good agreement with the desired performance metrics. For the desired diagnosis errors equal or less than 25%, 10%, 5.9%, and 2.5%, the CDS achieved diagnosis errors of 13.2%, 9.9%, 6.6%, and 4.6%, respectively. These diagnosis errors are achieved with acceptable false alarm rates [19] of 20.1%, 25%, 28.4%, and 54.7%, respectively. Therefore, we could simulate the flexibility and reliability of the proposed CDS for screening purposes even with a training dataset that is defective or tempered through a cyber-attack that may disrupt the labeling or remove some training patterns from the dataset.

In summary, a CDS for health screening application is proposed and implemented. This CDS incorporates decision-making trees, non-monotonic reasoning, a decision-making approach inspired from humans in the case of conflict-of-opinions, prediction using the extracted model, and the characteristics of non-Gaussian and non-linear health features. The CDS checks only one feature in each perception-multiple-action cycle, making the proposed algorithm simple and fast. Finally, this work is the second step for designing the ADMS for screening applications in a smart e-Health system that can be extended for different healthcare policies such as diagnosing the disease class, prevention and early detection.

REFERENCES

[1] An Architectural Blueprint for Autonomic Computing. (Jun. 2005) *IBM Autonomic Computing White Paper*. Accessed: May 1, 2021. [Online]. Available: https://www-03.ibm.com/autonomic/pdfs/AC%2Blueprint%20White%20Paper%20V7.pdf

[2] J. O. Kephart and D. M. Chess, "The vision of autonomic computing," *Computer*, vol. 36, no. 1, pp. 41–50, Jan. 2003.

[3] M. J. Deen, "Information and communications technologies for elderly ubiquitous healthcare in a smart home," *Pers. Ubiquitous Comput.*, vol. 19, nos. 3–4, pp. 573–599, Jul. 2015.

[4] S. Majumder, T. Mondal, and M. J. Deen, "Wearable sensors for remote health monitoring," *Sensors*, vol. 17, no. 1, pp. 130–175, 2017.

[5] H. Wang, N. Agoulmine, M. J. Deen, and J. Zhao, "A utility maximization approach for information-communication tradeoff in wireless body area networks," *Pers. Ubiquitous Comput.*, vol. 18, no. 8, pp. 1963–1976, Dec. 2014.

[6] H. Wang, "Information-based energy efficient sensor selection in wireless body area networks," in *Proc. IEEE Int. Conf. Commun.-Symp. Sel. Areas Commun. E-Health Track*, Kyoto, Japan, Jun. 2011, pp. 1–6,

[7] S. Majumder, E. Aghayi, M. Noferesti, H. Memarzadeh-Tehran, T. Mondal, Z. Pang, and M. J. Deen, "Smart homes for elderly healthcare-Recent advances and research challenges," *Sensors*, vol. 17, no. 11, pp. 2496–2528, 2017.

[8] J. M. Fuster, *Cortex and Mind: Unifying Cognition*. London, U.K.: Oxford Univ. Press, 2003.

[9] S. Feng, P. Setoodeh, and S. Haykin, "Smart home: Cognitive interactive people-centric Internet of Things," *IEEE Commun. Mag.*, vol. 55, no. 2, pp. 34–39, Feb. 2017.

[10] M. Naghshvarianjahromi, S. Kumar, and M. J. Deen, "Brain-inspired intelligence for real-time health situation understanding in smart e-Health home applications," *IEEE Access*, vol. 7, pp. 180106–180126, 2019.

[11] M. Naghshvarianjahromi, S. Kumar, and M. J. Deen, "Brain inspired dynamic system for the quality of service control over the long-haul nonlinear fiber-optic link," *Sensors*, vol. 19, no. 9, pp. 2175–2195, 2019.

[12] M. Naghshvarianjahromi, S. Kumar, and M. J. Deen, "Brain inspired dynamic system for the quality of service control over the long-haul nonlinear fiber-optic link," in *Proc. 16th Canadian Workshop Inf. Theory (CWIT)*, Hamilton, NY, Canada, Jun. 2019, pp. 1–5.

[13] M. Naghshvarianjahromi, S. Kumar, and M. J. Deen, "Smart long-haul fiber optic communication systems using brain like intelligence," *Proc. 16th Can. Workshop Inf. Theory (CWIT)*, Hamilton, ON, Canada, Jun. 2019, pp. 1–6.

[14] M. Naghshvarianjahromi, S. Kumar, and M. J. Deen, "Brain-inspired cognitive decision making for nonlinear and non-Gaussian environments," *IEEE Access*, vol. 7, pp. 180910–180922, 2019.

[15] M. Naghshvarianjahromi, S. Kumar, and M. J. Deen, "Natural brain-inspired intelligence for non-Gaussian and nonlinear environments with finite memory," *Appl. Sci.*, vol. 10, no. 3, pp. 1150–1177, 2020.

[16] S. Haykin, *Cognitive Dynamic Systems: Perception-Action Cycle, Radar, and Radio*. Cambridge, U.K.: Cambridge Univ. Press, 2012.

[17] N. F. Marko and R. J. Weil, "Non-Gaussian distributions affect identification of expression patterns, functional annotation, and prospective classification in human cancer genomes," *PLoS ONE*, vol. 7, no. 10, Oct. 2012, Art. no. e46935.

[18] R. Bono, M. J. Blanca, J. Arnau, and J. Gómez-Benito, "Non-normal distributions commonly used in health, education, and social sciences: A systematic review," *Frontiers Psychol.*, vol. 8, pp. 1–13, Sep. 2017.

[19] B. J. Drew, P. Harris, J. K. Zègre-Hemsey, T. Mammone, D. Schindler, R. Salas-Boni, Y. Bai, A. Tinoco, Q. Ding, and X. Hu, "Insights into the problem of alarm fatigue with physiologic monitor devices: A comprehensive observational study of consecutive intensive care unit patients," *PLoS ONE*, vol. 9, no. 10, Oct. 2014, Art. no. e110274.

[20] J. Henry, "Adoption of electronic health record systems among us non-federal acute care hospitals: 2008-2015," *ONC Data Brief*, no. 35, pp. 1–9, Oct. 2016.

[21] M. Ghassemi, T. Naumann, F. Doshi-Velez, N. Brimmer, R. Joshi, A. Rumshisky, and P. Szolovits, "Unfolding physiological state: Mortality modeling in intensive care units," in *Proc. KDD*, 2014, pp. 75–84.

[22] V. Gulshan, "Development and validation of a deep learning algorithm for detection of diabetic retinopathy in retinal fundus photographs," *J. Amer. Med. Assoc.*, vol. 316, no. 22, pp. 2402–2410, 2016.

[23] A. Esteva, B. Kuprel, R. A. Novoa, J. Ko, S. M. Swetter, H. M. Blau, and S. Thrun, "Dermatologist-level classification of skin cancer with deep neural networks," *Nature*, vol. 542, no. 7639, pp. 115–118, Feb. 2017.

[24] Y.-A. Chung and W.-H. Weng, "Learning deep representations of medical images using siamese CNNs with application to content-based image retrieval," in *Proc. Workshop Mach. Learn. Health (ML4H)*, 2017, pp. 1–5.

[25] K. Nagpal, D. Foote, Y. Liu, P.-H.-C. Chen, E. Wulczyn, F. Tan, N. Olson, J. L. Smith, A. Mohtashamian, J. H. Wren, G. S. Corrado, R. MacDonald, L. H. Peng, M. B. Amin, A. J. Evans, A. R. Sangoi, C. H. Mermel, J. D. Hipp, and M. C. Stumpe, "Development and validation of a deep learning algorithm for improving gleason scoring of prostate cancer," *NPJ Digit. Med.*, vol. 2, no. 1, pp. 1–11, Dec. 2019.

[26] A. Raghu, "Continuous state-space models for optimal sepsis treatment-a deep reinforcement learning approach," in *Proc. Mach. Learn. Healthcare (MLHC)*, 2017, pp. 1–17.

[27] W.-H. Weng, "Representation and reinforcement learning for personalized glycemic control in septic patients," in *Proc. NIPS*, 2017, pp. 1–8.

[28] M. Komorowski, L. A. Celi, O. Badawi, A. C. Gordon, and A. A. Faisal, "The artificial intelligence clinician learns optimal treatment strategies for sepsis in intensive care," *Nature Med.*, vol. 24, no. 11, pp. 1716–1720, Nov. 2018.

[29] E. P. Lehman, R. G. Krishnan, and X. Zhao, "Representation learning approaches to detect false Arrhythmia alarms from ECG dynamics," *Proc. Mach. Learn. Healthcare (MLHC)*, Stanford, CA, USA, Apr. 2018, pp. 1–15.
[30] T.-M. Hsu, "Unsupervised multimodal representation learning across medical images and reports," in *Proc. Workshop NeurIPS Mach. Learn. Health (ML4H)*, 2018, pp. 1–15.
[31] G. Liu, T. Hsu, M. McDermott, W. Boag, W. Weng, P. Szolovits, and M. Ghassemi, "Clinically accurate chest X-ray report generation," in *Proc. Mach. Learn. Healthcare (MLHC)*, 2019, pp. 1–20.
[32] S. Gehrmann, F. Dernoncourt, Y. Li, E. T. Carlson, and J. T. Wu, "Comparing deep learning and concept extraction based methods for patient phenotyping from clinical narratives," *PLoS One*, vol. 13, no. 2, 2018, Art. no. e0192360.
[33] L. Shen, L. R. Margolies, J. H. Rothstein, E. Fluder, R. McBride, and W. Sieh, "Deep learning to improve breast cancer detection on screening mammography," *Sci. Rep.*, vol. 9, no. 1, Dec. 2019, Art. no. 12495.
[34] A. C. Thompson, A. A. Jammal, and F. A. Medeiros, "A review of deep learning for screening, diagnosis, and detection of glaucoma progression," *Trans. Vis. Sci. Tech.*, vol. 9, no. 2, pp. 42–50, 2020.
[35] S. E. Miller, S. Thapa, A. L. Robin, L. M. Niziol, P. Y. Ramulu, M. A. Woodward, I. Paudyal, I. Pitha, T. N. Kim, and P. A. Newman-Casey, "Glaucoma screening in nepal: Cup-to-disc estimate with standard mydriatic fundus camera compared to portable nonmydriatic camera," *Amer. J. Ophthalmol.*, vol. 182, pp. 99–106, Oct. 2017.
[36] R. Zhao, X. Chen, X. Liu, Z. Chen, F. Guo, and S. Li, "Direct cup-to-disc ratio estimation for glaucoma screening via semi-supervised learning," *IEEE J. Biomed. Health Informat.*, vol. 24, no. 4, pp. 1104–1113, Apr. 2020.
[37] C. C. Owsley, "Diabetes eye screening in urban settings serving minority populations: Detection of diabetic retinopathy and other ocular findings using telemedicine," *JAMA Ophthalmol.*, vol. 133, no. 2, pp. 174–181, 2015.
[38] H. Abbas, F. Garberson, E. Glover, and D. P. Wall, "Machine learning for early detection of autism (and other conditions) using a parental questionnaire and home video screening," in *Proc. IEEE Int. Conf. Big Data (Big Data)*, Boston, MA, USA, Dec. 2017, pp. 3558–3561.
[39] H. Abbas, F. Garberson, E. Glover, and D. P. Wall, "Machine learning approach for early detection of autism by combining questionnaire and home video screening," *J. Amer. Med. Inform. Assoc.*, vol. 25, no. 8, pp. 1000–1007, Aug. 2018.
[40] L. E. K. Achenie, A. Scarpa, R. S. Factor, T. Wang, D. L. Robins, and D. S. McCrickard, "A machine learning strategy for autism screening in toddlers," *J. Develop. Behav. Pediatrics*, vol. 40, no. 5, pp. 369–376, 2019.
[41] B. Jin, T. Hoai Thu, E. Baek, S. Sakong, J. Xiao, T. Mondal, and M. J. Deen, "Walking-age analyzer for healthcare applications," *IEEE J. Biomed. Health Informat.*, vol. 18, no. 3, pp. 1034–1042, May 2014.
[42] P. Mandal, K. Tank, T. Mondal, C.-H. Chen, and M. J. Deen, "Predictive walking-age health analyzer," *IEEE J. Biomed. Health Informat.*, vol. 22, no. 2, pp. 363–374, Mar. 2018.
[43] N. Foulquier and A. Saraux. *Application of Machine Learning in Predicting Early Diagnosis of Rheumatic Diseases*. Accessed: May 1, 2021. [Online]. Available: https://rheumatology.medicinematters.com/diagnosis-and-screening/artificial-intelligence/machine-learning-diagnosis-rheumatic-disease/17437330#
[44] C. Cortes and V. Vapnik, "Support-vector networks," *Mach. Learn.*, vol. 20, no. 3, pp. 273–297, 1995.
[45] D. Silver, A. Huang, C. J. Maddison, A. Guez, L. Sifre, G. van den Driessche, J. Schrittwieser, I. Antonoglou, V. Panneershelvam, M. Lanctot, S. Dieleman, D. Grewe, J. Nham, N. Kalchbrenner, I. Sutskever, T. Lillicrap, M. Leach, K. Kavukcuoglu, T. Graepel, and D. Hassabis, "Mastering the game of go with deep neural networks and tree search," *Nature*, vol. 529, no. 7587, pp. 484–489, Jan. 2016.
[46] V. Novák, I. Perfilieva, and J. Moáko, *Mathematical Principles of Fuzzy Logic*. Dordrecht, The Netherlands: Kluwer, 1999.
[47] L. A. Zadeh, "Fuzzy sets," *Inf. Control*, vol. 8, no. 3, pp. 338–353, Jun. 1965.
[48] R. E. Bellman and L. A. Zadeh, "Decision-making in a fuzzy enviroment," *Manage. Sci.*, vol. 17, no. 4, p. 141, 1970.
[49] S. Voss, "Fuzzy logic in health care settings: Moral math for value-laden choices," *J. Humanistic Math.*, vol. 6, no. 2, pp. 161–178, Jul. 2016.
[50] J. H. T. Bates and M. P. Young, "Applying fuzzy logic to medical decision making in the intensive care unit," *Amer. J. Respiratory Crit. Care Med.*, vol. 167, no. 7, pp. 948–952, Apr. 2003.
[51] D. DeMazumder, D. E. Lake, A. Cheng, T. J. Moss, E. Guallar, R. G. Weiss, S. R. Jones, G. F. Tomaselli, and J. R. Moorman, "Dynamic analysis of cardiac rhythms for discriminating atrial fibrillation from lethal ventricular arrhythmias," *Circulat., Arrhythmia Electrophysiol.*, vol. 6, no. 3, pp. 555–561, Jun. 2013.
[52] A. Petränas, L. Sörnmo, and V. Marozas, "Detection of occult paroxysmal atrial fibrillation," *Med. Biol. Eng. Comput.*, vol. 53, no. 4, pp. 287–297, Apr. 2015.
[53] *The Top 10 Causes of Death*. Accessed: May 1, 2021. [Online]. Available: https://www.who.int/news-room/fact-sheets/detail/the-top-10-causes-of-death
[54] P. Harris and D. Lysitsas, "Ventricular arrhythmias and sudden cardiac death," *BJA Educ.*, vol. 16, no. 7, pp. 221–229, Jul. 2016.
[55] R. Mehra, "Global public health problem of sudden cardiac death," *J. Electrocardiol.*, vol. 40, no. 6, pp. S118–S122, Nov. 2007.
[56] National Heart, Lung, and Blood Institute. (Jul. 1, 2011). *Who Is at Risk for an Arrhythmia*. Accessed: May 1, 2021. [Online]. Available: http://www.nhlbi.nih.gov/health/health-topics/topics/arr/atrisk
[57] *Arrhythmia Treatment Services, Brigham Women's Hospital*. Accessed: May 1, 2021. [Online]. Available: https://www.brighamandwomens.org/heart-and-vascular-center/resources/Arrhythmia-treatment
[58] S. S. Padhi, "Prevalence of cardiac arrhythmias in a community based chiropractic practice," *J. Can. Chiropractic Assoc.*, vol. 58, no. 3, pp. 238–245, 2014.
[59] S. M. Pehrson, C. Blomström-LUNDQVIST, E. Ljungström, and P. Blomström, "Clinical value of transesophageal atrial stimulation and recording in patients with arrhythmia-related symptoms or documented supraventricular tachycardia-correlation to clinical history and invasive studies," *Clin. Cardiol.*, vol. 17, no. 10, pp. 528–534, Oct. 1994.
[60] T. Hendrikx, M. Rosenqvist, P. Wester, H. Sandström, and R. Hörnsten, "Intermittent short ECG recording is more effective than 24-hour holter ECG in detection of arrhythmias," *BMC Cardiovascular Disorders*, vol. 14, no. 1, pp. 14–41, Dec. 2014.
[61] Q. Zhang, X. Chen, Z. Fang, and S. Xia, "False arrhythmia alarm reduction in the intensive care unit using data fusion and machine learning," in *Proc. IEEE-EMBS Int. Conf. Biomed. Health Informat. (BHI)*, Las Vegas, NV, USA, Feb. 2016, pp. 232–235.
[62] *The PhysioNet Computing in Cardiology Challenge 2017*. Accessed: May 1, 2021. [Online]. Available: https://physionet.org/content/challenge-2017/1.0.0/
[63] G. D. Clifford, "AF classification from a short single lead ECG recording: The PhysioNet/computing in cardiology challenge 2017," in *Proc. Comput. Cardiol.*, Rennes, France, Sep. 2017, pp. 1–4.
[64] *Datta MATLAB Codes for Feature Extraction*. Accessed: May 1, 2021. [Online]. Available: https://physionet.org/content/challenge-2017/1.0.0/sources/shreyasi-datta-209.zip

MAHDI NAGHSHVARIANJAHROMI (Student Member, IEEE) received the M.S. degree in communications engineering from the Amirkabir University of Technology (AUT), in 2014, and the Ph.D. degree in electrical and computer engineering from McMaster University, Hamilton, Canada, in 2020. He is currently working as a Postdoctoral Fellow with the Department of Electrical and Computer Engineering, McMaster University. He published more than 38 articles. His current research interests include fiber-optic communications system and nonlinear impairment mitigation, smart home and automatic healthcare systems, computer sciences, statistical processing and brain-like intelligence, microwave imaging, cognitive dynamic systems, antennas, arrays, and RF devices.

SUMIT MAJUMDER (Graduate Student Member, IEEE) received the B.Sc. degree in electrical and electronic engineering from the Bangladesh University of Engineering and Technology, Dhaka, Bangladesh, in 2007, and the M.A.Sc. and Ph.D. degrees in electrical and computer engineering from McMaster University, Hamilton, Canada, in 2011 and 2020, respectively. He is currently working as a Research Engineer with the Department of Electrical and Computer Engineering, McMaster University. His research interests include wearable sensors, biomedical signal processing, tele-health monitoring, artificial intelligence, and machine learning.

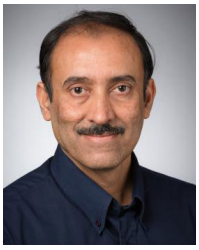

SHIVA KUMAR (Member, IEEE) received the M.S. and Ph.D. degrees in electrical communication engineering from the Indian Institute of Science, Bangaluru, India, in 1990 and 1994, respectively, and the Ph.D. degree in communications engineering from Osaka University, Japan, in 1997. He worked at Corning Incorporated, as a Senior Research Scientist, from 1998 to 2001, as a Supervisor, from 2001 to 2002, and then as a Research Associate, from 2002 to 2003. In 2003, he joined McMaster University, ON, Canada, where he is currently a Professor. He has authored a textbook *Fiber Optic Communications* (2014), edited a book *Nonlinear Fiber Optics* (2011), and published more than 80 articles in refereed journals and seven book chapters.

NARJES NAGHSHVARIANJAHROMI received the general practice Ph.D. degree from the Tabriz University of Medical Science, in 2011, and the M.D. degree in OBGYN. She did her residency of obstetrics and gynecology with the Shahid Beheshti University of Medical Sciences. She is currently an Assistant Professor with the Department of Obstetrics and Gynecology, Jahrom University of Medical Science, Jahrom, Iran.

M. JAMAL DEEN (Life Fellow, IEEE) is currently a Distinguished University Professor (highest rank of a Professor in Canada), a Senior Canada Research Chair in information technology, and the Director of the Micro- and Nano-Systems Laboratory, McMaster University. His research record includes more than 620 peer-reviewed articles (about 20% are invited), two textbooks *Silicon Photonics-Fundamentals and Devices* and *Fiber Optic Communications: Fundamentals and Applications*, 12 awarded patents of which six were extensively used in industry, and 21 Best Paper/Poster/Presentation Awards. His current research interests include nanoelectronics, optoelectronics, nanotechnology, data analytics, and their emerging applications to health and environmental sciences. He was elected as the President for the Academy of Science, Royal Society of Canada, for the term 2015–2017. He has also been elected as a Fellow status in 12 national academies and professional societies, including the Royal Society of Canada (the highest honor for academics, scholars and artists in Canada), the Canadian Academy of Engineering (the highest honor for engineers in Canada), the Chinese Academy of Sciences, American Physical Society (APS), and the Electrochemical Society (ECS). His awards and honors, include the Callinan Award and the Electronics and Photonics Award from the Electrochemical Society, the Humboldt Research Award from the Alexander von Humboldt Foundation, the Eadie Medal from the Royal Society of Canada, the McNaughton Gold Medal (highest award for engineers), the Fessenden Medal, and the Ham Education Medal (highest award for educators), all from IEEE Canada. In addition, he was awarded the four Honorary Doctorate degrees in recognition of his exceptional research and scholarly accomplishments, exemplary professionalism and value services. In July 2018, he was elected to the Order of Canada, the highest civilian honor awarded by the Government of Canada.